Advanced Control Technique for Islanded Microgrid based on H-Infinity Controller

First B. E. Sedhom ***Second M. M. El-Saadawi*** ***Third E-E. Abd-Raboh***
Faculty of engineering, Mansoura University, Egypt
eng_bishoy90@mans.edu.eg

Abstract: *This paper presents an advanced control method for islanded microgrids (MG). The proposed control method is based on H-infinity (H∞) controller. The method is applied to regulate the system frequency and voltage to allowable range against the disturbances caused by load variations and meanwhile improve the system power quality. To prove how efficient is the proposed controller, it is compared with two other controllers including a base V-f controller and a conventional droop controller. The V-f control method consists of two control loops to control the voltage source inverter (VSI). The conventional control method applies a droop control with the V-f control method to improve its performance. The proposed control method is based on H∞ to modify the operation of the conventional control method. The three controllers are applied to a test system simulated in Matlab/Simulink environment for two case studies. The first one is a MG supplying linear loads (i.e. no harmonics effect), whereas the other one is a MG supplying nonlinear loads. The results prove that the proposed control method is more efficient than the other two methods in adjusting the system voltage and frequency of the islanded MG against the disturbances caused by load variations. It can also improve the system power quality by reducing the THD of current and voltage waveforms.*

Keywords: *Microgrid, V-f control, Droop control, H-infinity, Voltage control, Frequency control.*

1. Introduction

Nowadays microgrids have emerged as one of the most effective options for satisfying the ever-increasing energy demand [1]. A microgrid (MG) is a small-scale power grid operates independently or in conjunction with the area's main electrical grid. It is a discrete energy system consisting of distributed generations (DGs), battery storage and loads. MGs have many advantages as they can reduce pollution, increase system flexibility, reduce transmission and distribution power losses and generally they can provide effective support to utility grids [2]. One of the major challenges facing MGs operators is the question of how to control them under different operating modes [3]. MGs can operate in either grid connected or islanded modes. In grid connected mode, the MG voltage and frequency should be synchronized with the utility grid. In this case, the control system is used for synchronizing the utility grid with DG sources in order to regulate active reactive power control through voltage and frequency control [4]. In islanded mode, the MG operates autonomously when it is disconnected from the main grid. In this mode, the control method is applied to adjust the MG voltage and frequency to their acceptable limits to prevent MG instability [5].

Many control methods have been employed to regulate voltage and frequency of MGs in islanded mode. These methods include V/f control, P/Q control, droop control, peer to peer control, hierarchical control, PI/PID control, sliding mode control, master-slave control and distributed control method [4,6-8]. V/f control is a flexible and modular method that provides expandability and redundancy. Several papers in the literature have applied V/f control method for controlling voltage and frequency of islanded MG [9-13]. Authors in [9-10] applied V/f control with the maximum power point tracking (MPPT) to regulate system voltage and frequency. Whereas, authors in [11-13], applied V/f control to achieve soft transition between grid-connected and islanded mode. However, the V/f control method is suffering from slow response and it can't restore the system voltage and frequency to their nominal values.

Droop control is the basic control method for load current sharing in MG applications. The method is traditionally adopted to distribute active and reactive power among the DGs operating in parallel. The droop control is simple as it is a decentralized control method where each input is paired with one output and it depends only on local information of the DGs. It has also a low cost and it doesn't need any communication between DG units [14]. Droop controller is applied for many applications in power systems. It can be used to: improve the system voltage unbalance [15], regulate the system voltage and frequency [16], achieve frequency stability [14], and achieve energy management [17]. However, the method requires a supplementary control to restore the system voltage and frequency to their nominal values [18].

H-Infinity (H∞) is a repetitive control method used to synthesize the controller to provide fast stabilization with better performance. It has the power to solve multi-objectives and multivariate systems. To apply this technique, the control problem must be transferred firstly to a mathematical optimization problem [19 - 23].

Hornik et al. [19] introduced a control system based on H∞ to ensure a pure sinusoidal current injected to a MG supplying nonlinear and unbalanced loads. The proposed control system has improved the tracking performance and reduced the total harmonic distortion (THD). Sheela et al. [20] applied H∞ algorithm to minimize voltage and frequency deviations after load changing. Baghaee et al. [21] presented a generalized descriptor system H∞ approach to enhance the performance of the H∞ controller for voltage source converters (VSC) based MG. Lam et al. [22] presented a robust H∞ control method for primary frequency control in standalone MGs. A multi-variable H∞ controller using a linear matrix inequalities (LMI) technique was designed and discussed in the paper and a μ-synthesis analysis was applied to ensure the system robustness. Jian et al. [23] applied H∞ controller to reduce the frequency fluctuations due to integrating DGs with a MG. They have used the particle swarm optimization (PSO) technique to improve the system performance by optimizing the weighting function of the controller.

The H∞ control method is one of the most advanced techniques available today for designing robust controllers. One great advantage with this method is that it allows the designer to tackle the most general form of control architecture wherein explicit accounting of uncertainties, disturbances, and performance measures can be accomplished [24]. The method can be applied for many applications in power management and control of MGs in both grid-connected and isolated modes [25-31].

Nagahara et al. [25] applied H∞ controller to ensure a power balance and reduce the frequency fluctuations. Dou et al. [26] and Jankovic et al. [27] applied H∞ controller to adjust the current and voltage in the DC–AC interface of micro-sources in MGs. The H∞ controller was used to improve the power quality and to reduce THD in MG in [28]. Sedghi et al. [29] proposed an H∞ based control method to adjust the MG under the uncertainties of the load changes. Lam et al. [30] applied H∞ control method to regulate the frequency fluctuations in MG whereas, Hornik et al. [31] proposed a control method based on H∞ repetitive controller to adjust the grid tied inverters.

The power quality of the distribution networks is greatly affected, by the increasing use of renewable energy resources which employ power electronic devices to regulate their output. The power quality is mainly measured based on the THD. Both power electronic devices and non-linear loads consume non-sinusoidal currents and hence increase the total harmonic distortion (THD) in MGs [32]. The increased THD results in MG overheating, system instability, transmission and distribution losses increasing and protection system failure [33]. To reduce the THD to its acceptable limits, filters are applied for harmonic mitigation. Voltage source inverter (VSI) is usually interfaced with LCL filter to mitigate the THD in output currents [34]. The maximum allowable THD for both wind and PV connected to the utility grid is 5% according to IEEE std. 519-1992 [35].

This paper presents an advanced control technique based on H∞ controller for islanded MG. The main objective of the proposed method is: (i) adjust the system voltage and frequency and (ii) improve the system power quality. The proposed method is a repetitive control one as it uses the internal model in H∞ control. The method is also an adaptive and robust one as it applies different weighting parameters with the H∞ control method. The method is represented in Matlab/Simulink environment and verified using a test system under two different loading conditions using linear and non-linear load. A comparison between both V/f control, conventional droop control and the proposed control method is presented to explain the effectiveness and efficiency of the method.

The rest of the paper is organized as follow; section 2 introduces the V/f control method, section 3 presents the conventional control method, section 4 introduces the state space model representation, section 5 presents the proposed control method, and section 6 introduces the case studies. Finally, section 7 concludes the paper.

2. V/f Control Method

This control method is applied to control the MG parameters under the islanded mode of operation only. In this mode, it is required to control MG voltage and frequency within their acceptable limits to meet all load requirements. This control method is very important during transition between off-grid and on-grid mode. [2, 4, 6]. The method is consisting of two control loops. The first is the voltage control loop that is applied to provide the reference current for the VSI. The second is the current control loop which provides

the reference voltage to the VSI. The equations represent the two control loops are explained in the following subsections.

2.1. Voltage Controller

The voltage controller's Differential Algebraic Equations (DAEs) are expressed as [36-38]:

$$\dot{\emptyset}_{q_i} = V_{q_i}^* - V_{q_i} \quad (1)$$

$$\dot{\emptyset}_{d_i} = V_{d_i}^* - V_{d_i} \quad (2)$$

$$i_{ld_i}^* = F_i i_{d_i} - \omega C_{f_i} V_{q_i} + K_{PV_i}\left(V_{d_i}^* - V_{d_i}\right) + K_{IV_i}\emptyset_{d_i} \quad (3)$$

$$i_{lq_i}^* = F_i i_{q_i} - \omega C_{f_i} V_{d_i} + K_{PV_i}\left(V_{q_i}^* - V_{q_i}\right) + K_{IV_i}\emptyset_{q_i} \quad (4)$$

Where $\emptyset_{d_i}$ and $\emptyset_{q_i}$ are the state variables defined for PI controllers, K's are the integrator gain factors, and ω is the nominal angular frequency. Figure 1 shows a block diagram of this control loop.

2.2. Current Controller

The current controller DAEs are expressed as [36-38]:

$$\dot{\gamma}_{q_i} = i_{lq_i}^* - i_{lq_i} \quad (5)$$

$$\dot{\gamma}_{d_i} = i_{ld_i}^* - i_{ld_i} \quad (6)$$

$$V_{id_i}^* = -\omega L_{f_i} i_{lq_i} + K_{PC_i}\left(i_{ld_i}^* - i_{ld_i}\right) + K_{IC_i}\gamma_{d_i} \quad (7)$$

$$V_{iq_i}^* = -\omega L_{f_i} i_{ld_i} + K_{PC_i}\left(i_{lq_i}^* - i_{lq_i}\right) + K_{IC_i}\gamma_{q_i} \quad (8)$$

Where γ_{d_i} and γ_{q_i} are the state variables defined for PI controllers, K's are the integrator gain factors, and i_{ld_i} and i_{lq_i} are the direct and quadrature components of i_{l_i}. Figure 2 illustrates a block diagram of the current control loop.

3. Conventional Control Method

The conventional control method is proposed and simulated to control MGs in islanded mode. The controller is composed of three loops. The first one is the droop control used to provide the active and reactive power references during MG islanded mode. The second and third loops are the voltage and current control loops [39-40]. To improve the system power quality, the VSI voltage output is filtered through LCL filter as it contains a large number of harmonic orders [41].

This control method is based on the relationship between active power with frequency and reactive power with voltage. According to droop characteristics, an increase in active power output leads to a decrease in load angle and hence a decrease in the frequency. Similarly, any increase in reactive power output leads to a reduction in terminal voltage. This control is a decentralized one as it uses only the local information of the DGs. In addition to its low cost, the main advantage of this method is that it doesn't need any communication links between DG units. The droop control method can be expressed mathematically as follow;

Firstly, the instantaneous active and reactive power p and q generated by the ith VSI, are calculated according to the output voltage and current; then a low pass filter is used to eliminate the high frequency components [36-38].

$$p = \left(v_{\mathrm{od}} i_{od} + v_{\mathrm{oq}} i_{\mathrm{oq}}\right) \quad (9)$$

$$q = \left(v_{\mathrm{od}} i_{\mathrm{oq}} - v_{\mathrm{oq}} i_{od}\right) \quad (10)$$

Where $V_{\mathrm{od}}, V_{\mathrm{oq}}$, i_{od}, and i_{oq} are the direct and quadratic components of the voltage and current, respectively. To obtain the fundamental active and reactive power P and Q, the filter is applied to the instantaneous power in (9) and (10).

$$P = \frac{\omega_c}{S+\omega_c}\, p \quad (11)$$

$$Q = \frac{\omega_c}{S+\omega_c}\, q \quad (12)$$

Where ω_c rad/s is the cut-off frequency of the low pass filter, and '*S*' denotes Laplace transformation. The droop control method can be expressed mathematically as:

$$\omega^* = \omega_{ref} - m_p(P) \quad (13)$$

$$v_{od}{}^* = v_{ref} - n_q(Q) \quad (14)$$

$$v_{oq}{}^* = 0 \quad (15)$$

Where ω* is the grid angular frequency, ω_{ref} and v_{ref} are the frequency and voltage references, v_{od}* and v_{oq}* are the d-axis and q-axis voltage and m_p and n_q are the slopes of the droop characteristics.

Figure 3 shows a block diagram of the droop controller whereas, Fig. 4 shows a Simulink representation of the proposed conventional controller

4. State space model representation

In this paper, different control loops are proposed to control both voltage and frequency and meanwhile improve power quality in an islanded MG. Firstly, a droop controller is applied to provide the reference voltage and frequency after calculating the required MG power. In this controller, the instantaneous active and reactive power p_{gi} and q_{gi} generated by the ith VSI are calculated according to the output voltage and current. A low pass filter is added to obtain the fundamental active and reactive power. Then the droop controller is applied to obtain the reference voltage and frequency. Secondly, the voltage and current are adjusted using both voltage and current control loops. Thirdly, the inverter output voltage waveform is regulated using a coupling circuit to eliminate the higher frequency harmonic orders. The mathematical equations of these control loops are handled in *d-q* reference frame.

The state space models of the above control loops are used to obtain a complete model of the inverter. The following equations represent the inverter

complete model that obtained according to equations from (1) to (15).

$$[\dot{x_{invi}}] = A_{invi}[x_{invi}] + B_{invi1}\begin{bmatrix}\omega_{ref}\\ v_{ref}\end{bmatrix} + B_{invi2}\begin{bmatrix}v_{idi}\\ v_{iqi}\\ v_{bdi}\\ v_{bqi}\end{bmatrix} \quad (16)$$

$$[y_{invi}] = C_{invi}[x_{invi}] + D_{invi1}\begin{bmatrix}\omega_{ref}\\ v_{ref}\end{bmatrix} + D_{invi2}\begin{bmatrix}v_{idi}\\ v_{iqi}\\ v_{bdi}\\ v_{bqi}\end{bmatrix} \quad (17)$$

Where;

$x_{invi} =$

$$\begin{bmatrix}\delta_i & P_i & Q_i & \emptyset_{di} & \emptyset_{qi} & \gamma_{di} & \gamma_{qi} & i_{ldi} & i_{lqi} & v_{odi} & v_{oqi} & i_{odi} & i_{oqi}\end{bmatrix}^T$$

$A_{invi} =$

$$\begin{bmatrix}
0 & -m_p & 0 & 0 & 0 & 0 & 0 & 0 & 0 & 0 & 0 & 0\\
0 & -\omega_c & 0 & 0 & 0 & 0 & 0 & 0 & \frac{1}{2}\omega_c i_{od} & \frac{1}{2}\omega_c i_{oq} & \frac{1}{2}\omega_c v_{od} & \frac{1}{2}\omega_c v_{oq}\\
0 & 0 & -\omega_c & 0 & 0 & 0 & 0 & 0 & \frac{1}{2}\omega_c i_{oq} & -\frac{1}{2}\omega_c i_{od} & -\frac{1}{2}\omega_c v_{oq} & \frac{1}{2}\omega_c v_{od}\\
0 & 0 & -n_q & 0 & 0 & 0 & 0 & 0 & -1 & 0 & 0 & 0\\
0 & 0 & 0 & 0 & 0 & 0 & 0 & 0 & 0 & -1 & 0 & 0\\
0 & 0 & -K_{pv}n_q & K_{iv} & 0 & 0 & 0 & -1 & 0 & -K_{pv} & -\omega_n C_f & F & 0\\
0 & 0 & 0 & 0 & K_{iv} & 0 & 0 & 0 & -1 & -\omega_n C_f & -K_{pv} & 0 & F\\
0 & 0 & 0 & 0 & 0 & 0 & 0 & -\frac{r_f}{L_f} & \omega_n & -\frac{1}{L_f} & 0 & 0 & 0\\
0 & 0 & 0 & 0 & 0 & 0 & 0 & -\omega_n & -\frac{r_f}{L_f} & 0 & -\frac{1}{L_f} & 0 & 0\\
0 & 0 & 0 & 0 & 0 & 0 & 0 & \frac{1}{C_f} & 0 & 0 & \omega_n & -\frac{1}{C_f} & 0\\
0 & 0 & 0 & 0 & 0 & 0 & 0 & 0 & \frac{1}{C_f} & -\omega_n & 0 & 0 & -\frac{1}{C_f}\\
0 & 0 & 0 & 0 & 0 & 0 & 0 & 0 & 0 & \frac{1}{L_c} & 0 & -\frac{r_c}{L_c} & \omega_n\\
0 & 0 & 0 & 0 & 0 & 0 & 0 & 0 & 0 & 0 & \frac{1}{L_c} & -\omega_n & -\frac{r_c}{L_c}
\end{bmatrix}$$

$B_{invi1} =$

$$\begin{bmatrix}
1 & 0\\
0 & 0\\
0 & 0\\
0 & 1\\
0 & 0\\
0 & K_{pv}\\
0 & 0\\
0 & 0\\
0 & 0\\
0 & 0\\
0 & 0\\
0 & 0
\end{bmatrix}$$

$B_{invi2} =$

$$\begin{bmatrix}
0 & 0 & 0 & 0\\
0 & 0 & 0 & 0\\
0 & 0 & 0 & 0\\
0 & 0 & 0 & 0\\
0 & 0 & 0 & 0\\
0 & 0 & 0 & 0\\
0 & 0 & 0 & 0\\
\frac{1}{L_f} & 0 & 0 & 0\\
0 & \frac{1}{L_f} & 0 & 0\\
0 & 0 & 0 & 0\\
0 & 0 & 0 & 0\\
0 & 0 & -\frac{1}{L_c} & 0\\
0 & 0 & 0 & -\frac{1}{L_c}
\end{bmatrix}$$

$$[y_{invi}] = \begin{bmatrix}e_1\\ e_2\\ e_3\\ e_4\\ e_5\\ e_6\end{bmatrix} = \begin{bmatrix}\omega_{ref} - \omega^*\\ v_{ref} - v_{od}{}^*\\ v_{od}^* - v_{od}\\ v_{oq}^* - v_{oq}\\ i_{ld}^* - i_{ld}\\ i_{lq}^* - i_{lq}\end{bmatrix}$$

$C_{invi} =$

$$\begin{bmatrix}
0 & m_p & 0 & 0 & 0 & 0 & 0 & 0 & 0 & 0 & 0 & 0\\
0 & 0 & n_q & 0 & 0 & 0 & 0 & 0 & 0 & 0 & 0 & 0\\
0 & 0 & -n_q & 0 & 0 & 0 & 0 & 0 & 0 & -1 & 0 & 0\\
0 & 0 & 0 & 0 & 0 & 0 & 0 & 0 & 0 & 0 & -1 & 0\\
0 & 0 & -\omega_n C_f & K_{iv} & 0 & 0 & 0 & -1 & 0 & 0 & -\omega_n C_f & F & 0\\
0 & 0 & 0 & 0 & K_{iv} & 0 & 0 & 0 & -1 & -\omega_n C_f & -K_{pv} & 0 & F
\end{bmatrix}$$

$$D_{invi1} = \begin{bmatrix}0 & 0\\ 0 & 0\\ 1 & 0\\ 0 & 0\\ 0 & K_{pv}\\ 0 & 0\end{bmatrix} \quad D_{invi2} = 0$$

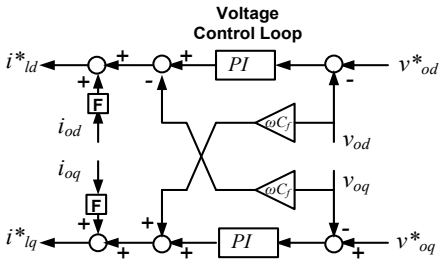

Fig. 1. Voltage control loop

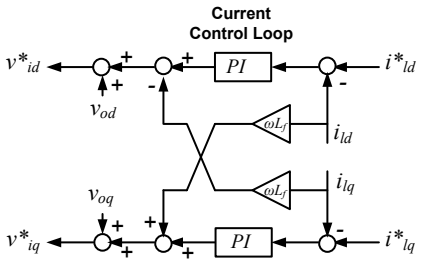

Fig. 2. Current control loop

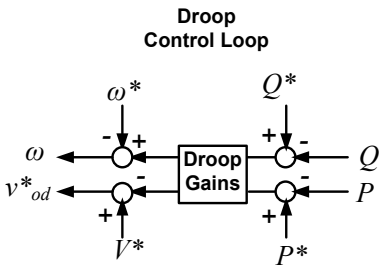

Fig. 3. Droop controller

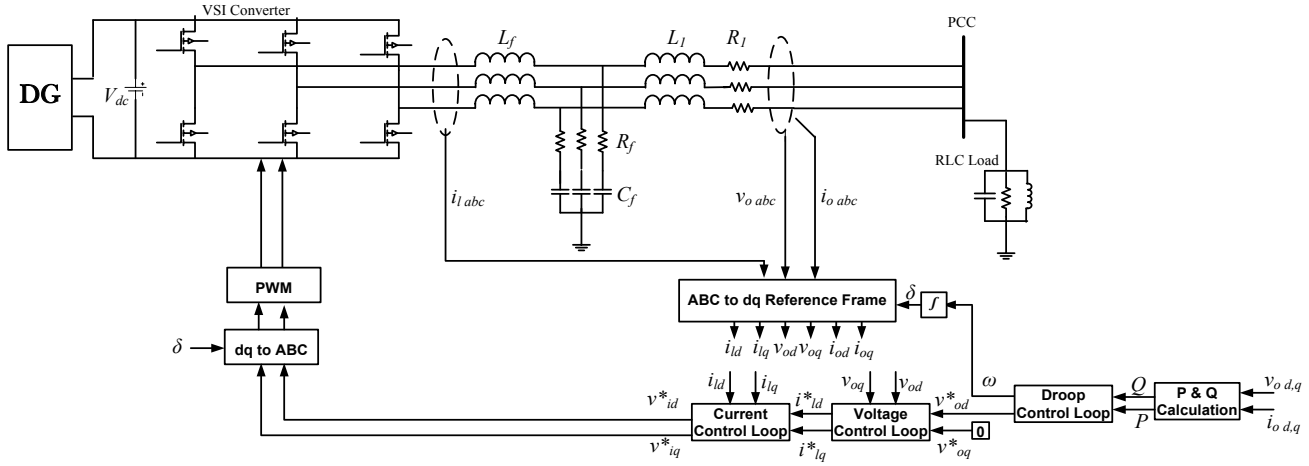

Fig. 4. The complete control system

The corresponding plant P can be employed as:

$$P = [D_{invi1} \quad D_{invi2}] + C_{invi}(sI - A_{invi})^{-1}[B_{invi1} \quad B_{invi2}] \tag{18}$$

Hence, the plant P is represented by the following state equation:

$$P = \left[\begin{array}{c|cc} A_{invi} & B_{invi1} & B_{invi2} \\ \hline C_{invi} & D_{invi1} & D_{invi2} \end{array}\right] \tag{19}$$

The last two control equations can be applied to control voltage and frequency for any MG containing DG units in islanded mode.

5. Proposed Control Method

Although the droop controller does not need any communication link between the DGs, it has its own disadvantages which limits the proper operation of MGs. The main disadvantage of this controller is the deviation od frequency and voltage from the nominal values when adjusting power sharing between DGs. To improve the conventional control response, this paper proposes a new control method depending on integrating $H\infty$ as a repetitive control with the conventional droop controller. The proposed $H\infty$ method consists of an inner voltage control loop and an outer current control loop to improve the system performance. The method is effective in enhancing the transient stability under the presence of uncertainties. It can significantly decrease the effect of perturbations on the control system. Figure 5(a) shows a schematic diagram of the control system using $H\infty$ method, where P represents the plant nominal transfer function and C represents feedback control. The internal model M shown in Fig. 5(a) has infinite dimension and consists of a low-pass filter $W(s)$ defined by (20) and cascaded with a delay line $e^{-T_d s}$ [19]. It is capable of generating periodic signals of a given fundamental period T_d; therefore, it has the ability to track periodic references and reject periodic disturbances having the same period. This provides a repetitive control scheme which covers a wide range of frequencies. The delay time T_d should be slightly lesser than the fundamental period T and can be computed using (21) [19].

$$W(s) = \frac{\omega_c}{s + \omega_c} \tag{20}$$

$$T_d = T - \frac{1}{\omega_c} \tag{21}$$

Where ω_c is the cut-off frequency of the low pass filter W.

The H-infinity controller, shown in Fig. 5(b), is designed for voltage and current control loops. To ensure the system stability, two weighting parameters ξ and μ are presented after estimated next to the open of the internal model feedback loop. The weighting parameters are applied to provide more freedom in the design. The closed loop system can be represented as follow:

$$\begin{bmatrix} \tilde{z} \\ \tilde{y} \end{bmatrix} = \tilde{P} \begin{bmatrix} \tilde{w} \\ u \end{bmatrix} \qquad u = C\tilde{y}$$

where, the $\tilde{P}$ is the extended plant and C is the controller to be designed. The extended plant $\tilde{P}$ includes the original plant P, the low pass filter W and the weighted parameters ξ and μ. The low pass filter is represented as follow;

$$W = \left[\begin{array}{c|c} A_w & B_w \\ \hline C_w & D_w \end{array}\right] = \left[\begin{array}{c|c} -\omega_{c1} & \omega_{c1} \\ \hline 1 & 0 \end{array}\right]$$

The generalized plant realizing is then obtained in (22) as it is shown in Fig. 5(b).

$$\tilde{P} = \left[\begin{array}{cccc:c} A_{invi} & 0 & 0 & B_{invi1} & B_{invi2} \\ B_w C_{invi} & A_w & B_w\xi & B_w D_{invi1} & B_w D_{invi2} \\ D_w C_{invi} & C_w & D_w\xi & D_w D_{invi1} & D_w D_{invi2} \\ 0 & 0 & 0 & 0 & \mu \\ \hdashline C_{invi} & 0 & \xi & D_{invi1} & D_{invi2} \end{array}\right] \tag{22}$$

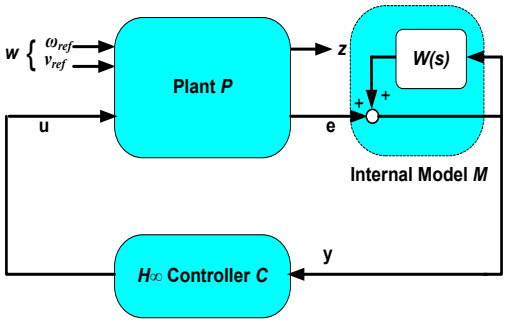

Fig. 5(a) Model structure of a control system using H∞ repetitive control

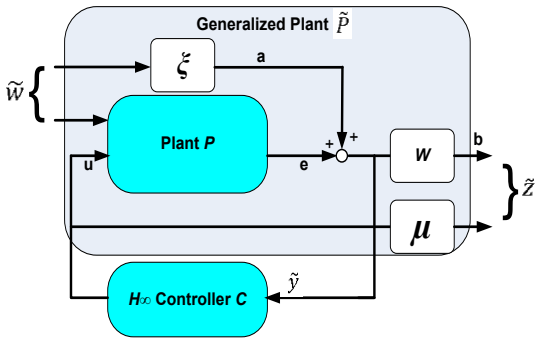

Fig. 5(b). H∞ controller with weighting parameters

Fig. 5. Formulation of the proposed controller

6. Case Study

In this case study, the three control systems are applied to a hypothetical MG consists of three DGs and three loads. The MG is connected to the main grid through a grid breaker for transition between grid-connected and islanded mode. Figure 6 shows a Simulink representation of this test system. The system parameters used in simulation are given in Table 1.

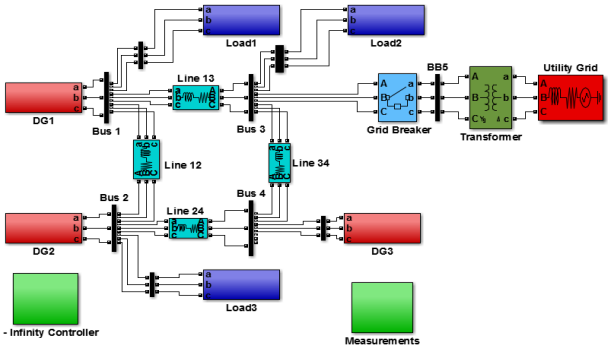

Fig. 6 Simulink representation of test system

TABLE 1. SYSTEM PARAMETERS

Components	*Parameters*	*Symbols*	*Quantity*
DG system	Nominal frequency	f	50 Hz
	Nominal RMS phase voltage	V	600 V
Converter LC filter	Inductance	L	5.42 mH
	Capacitance	C	11 μF
Controller	Frequency droop characteristics	K_p	0.0000042
	Voltage droop characteristics	K_Q	0.000177

6.1. Case 1: A MG supplying linear loads (No harmonics effect)

In this case, the test system is integrated to linear loads of RLC load connected at buses 1, 2 and 3 in Fig. 6. The three controllers are applied consecutively to the test system and the results are analyzed.

6.1.1. Applying V/f control method

The V/f controller is applied to the test system connected to a linear load shown in Fig. 7-a. The simulation results of this case study are explained in Figs. 8 and 9. The system voltage, current and frequency are shown in the left side of Fig. 8. A fast Fourier transform is done to the current and voltage waveforms to detect the value of the THD. The THD for both current and voltage waveforms are 2.04 % and 2.06 % respectively, as shown in the left side of Fig. 9.

6.1.2. Applying conventional control method

The conventional controller, explained in section 3, is applied to the test system with linear loads and the results are explained in Figs. 10 and 11. The system output voltage, current and frequency are shown in the left side of Fig. 10. The FFT analysis of the current and voltage waveforms are shown in the left side of Fig. 11. The THD of the load current is 0.93% and the THD of the load voltage is 1.93%.

6.1.3. Applying the proposed H∞ control method

The proposed H∞ controller, explained in section 5, is applied to the test system using *hinfsyn* algorithm and the results are explained in Figs. 12 and 13. The system output voltage, current and frequency are shown if the left side of Fig. 12. Whereas, the FFT analysis of the current and voltage waveforms are shown in the right side of Fig. 13. The THD of the load current and voltage are 0.65% and 1.27% respectively.

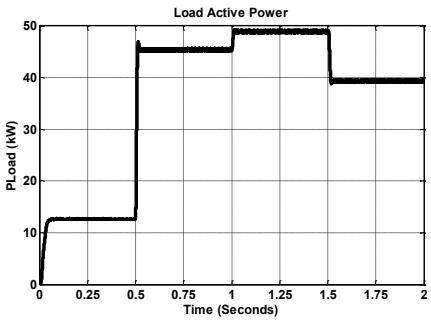

Load active power for case1

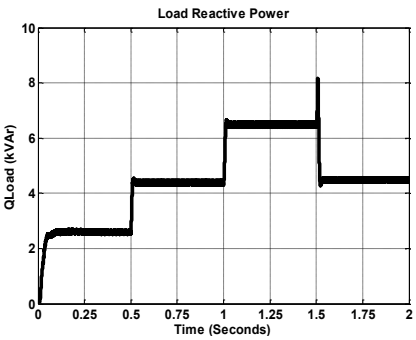

Load Reactive power for case 1

Fig. 7 (a) linear load curves

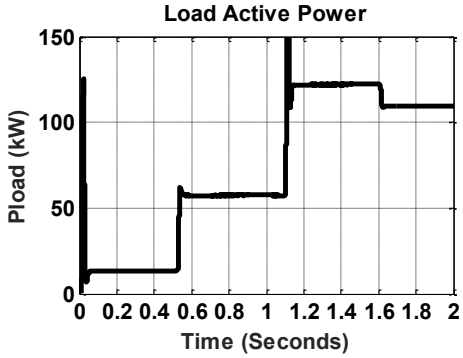

Load active power for case 2

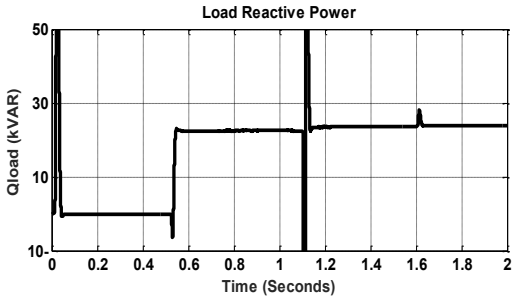

Load reactive load power for case 2

Fig. 7 (b) Non-linear load curves

Fig. 7. Load curves for the two case studies

6.1.4. Comparison between the three control methods for case 1

As explained in the above sections, the left-hand side of figures 8, 10 ,12 expresses the output waveforms obtained by applying the three controllers. On other hands, the left-hand side of figures 9, 11 ,13 depicts the FFT analysis of current and voltage waveforms after applying the three controllers. Out of the above results one can observe that:

- The conventional controller is better than V/f controller in adjusting system voltage and frequency to acceptable limits.
- Although the conventional controller reduces the ripples in the voltage, current and frequency waveforms, but it can't really adjust the system voltage and frequency to their nominal values after load variations.
- The proposed H∞ repetitive controller has a faster response and it can adjust the system voltage and frequency to their nominal values after any load variations (Fig. 12).
- The proposed control method is better than the two other methods in improving the system power quality by reducing THD for both current and voltage waveforms. A comparison between the current and voltage THD of the three controllers is shown in Table 2.

In general, the results prove that the proposed control method is more efficient than the other two methods in adjusting the system voltage and frequency of the islanded MG against the disturbances caused by load variations.

TABLE 2. Comparison between THD for case 1

	V/f control Method	Conventional Control Method		Proposed Control Method	
	% age value	% age value	% decrease	% age value	% decrease
THD_I	2.04	0.93	54.41%	0.65	68.13%
THD_V	2.06	1.93	6.31%	1.27	38.34%

6.2. Case 2: A MG supplying nonlinear loads

In this case, the test system is integrated to three similar nonlinear loads connected at buses 1, 2 and 3 in Fig. 6. Each load is composed of a three-phase uncontrolled rectifier loaded with an RLC. The active and reactive load curves are shown in Fig. 7-b. Again, the three controllers are applied consecutively to the test system for this case study and the results are analyzed.

6.2.1. Applying V/f controller

The simulation output voltage, current and frequency are shown in the right side of Fig. 8. The FFT analysis of the current and voltage waveforms are shown in the left side of Fig. 9. The THD of load current is 3.85% and that of the load voltage is 3.16%.

6.2.2. Applying conventional controller

The system output voltage, current and frequency are shown in the right side of Fig. 10. The FFT analysis of the current and voltage waveforms are shown in the left side of Fig. 11. The THD of load current is 2.03% and the THD of load voltage is 2.30%.

6.2.3. Applying proposed H∞-based controller

The proposed multi-stage H∞ controller is applied to the test system using *hinfsyn* algorithm. The system output voltage, current and frequency are shown if the right side of Fig. 12. The FFT analysis of the current and voltage waveforms are shown in the right side of Fig. 13. The THD of the load current is 0.89% and the THD of the load voltage is 1.50%.

6.2.4. Comparison between the three controllers for case 2

For this case study, the results represent the output waveforms obtained by applying the three control methods are presented in the right-hand side of Figs. 8, 10, and 12. The FFT analysis of current and voltage waveforms after applying the three controllers are expressed in Figs. 9, 11, and 13. Out of the above results it can be concluded that:

- Unlike the first case study, integrating non-linear loads to the islanded MG test system causes interruptions in system voltage, current and frequency.
- Both V/f and conventional controllers can't adjust system voltage, current and frequency for this case (due to the presence of non-linear loads).
- Once more, the conventional controller is better than V/f controller in adjusting system voltage and frequency to acceptable limits.
- However, using the proposed H∞ controller improves the system voltage, current and frequency. The method is capable of improving the system power quality better than the other two controllers.
- A comparison between the current and voltage THD of the three controllers are shown in Table 3.

TABLE 3. Comparison between THDs for case 2

	V/F control	Traditional Control Method		Proposed Control Method	
	% age value	% age value	% decrease	% age value	% decrease
THD_I	3.85	2.03	47.27%	0.89	76.88%
THD_V	3.16	2.30	27.21%	1.50	52.53%

V/f Control Method

Case 1(Without non-linear load) **Case 2 (With non-linear load)**

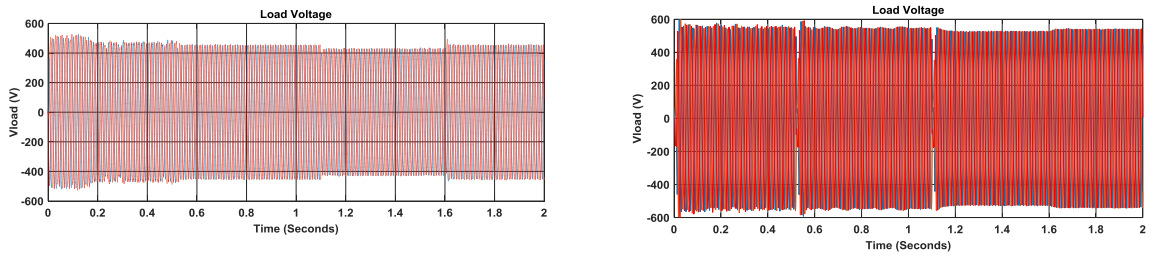

Fig. 8(a) Load voltage

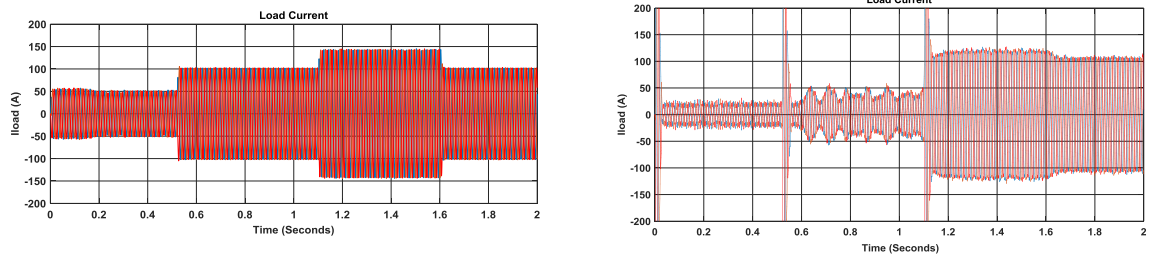

Fig. 8(b) Load current

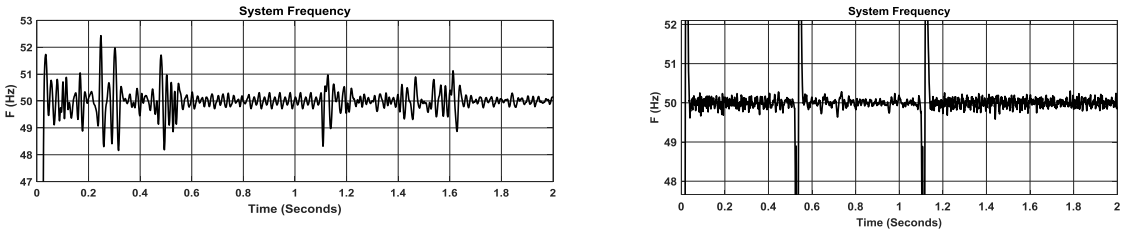

Fig. 8(c) System frequency

Fig. 8. Results for the V/f control method

V/f Control Method

Case 1(Without non-linear load) **Case 2 (With non-linear load)**

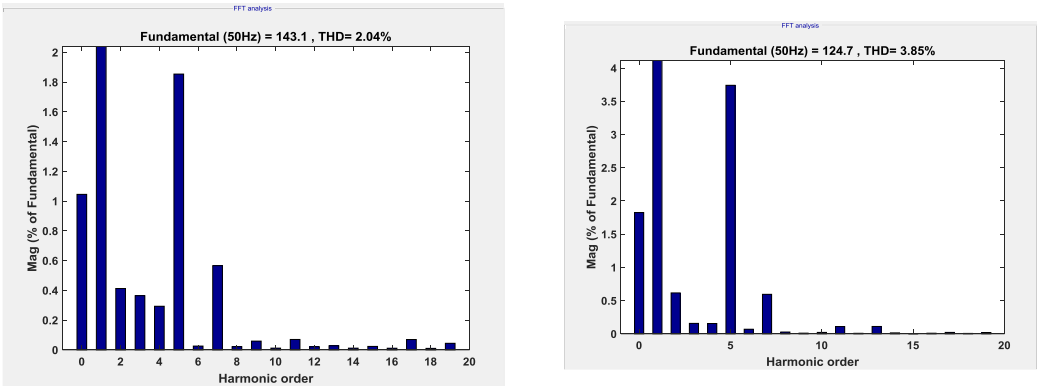

Fig. 9(a) FFT analysis for the load current waveform

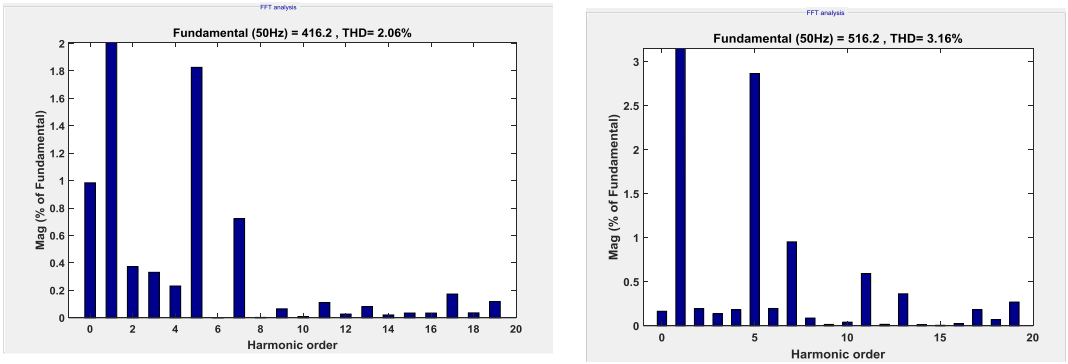

Fig. 9(b) FFT analysis for the load voltage waveform

Fig. 9. FFT analysis of current and voltage waveforms using V/f control method

Conventional Control Method

Case 1(Without non-linear load) **Case 2 (With non-linear load)**

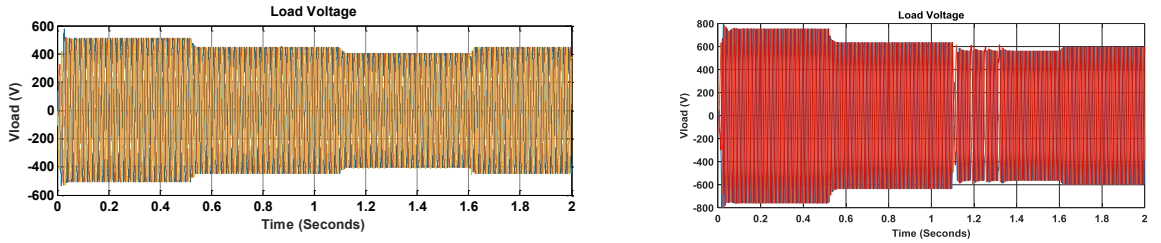

Fig. 10(a) Load voltage

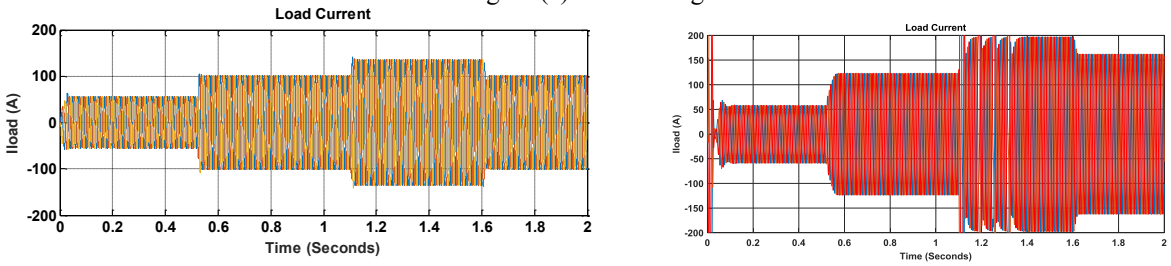

Fig. 10(b) Load current

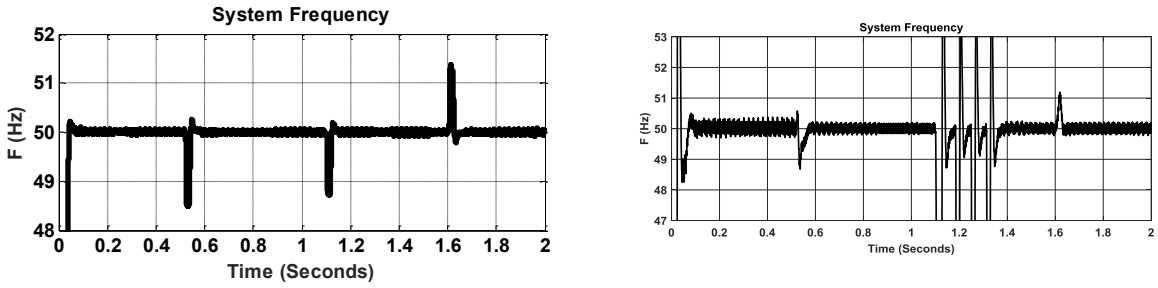

Fig. 10(c) System frequency

Fig. 10. Results for conventional control method

Conventional Control Method

Case 1(Without non-linear load) **Case 2 (With non-linear load)**

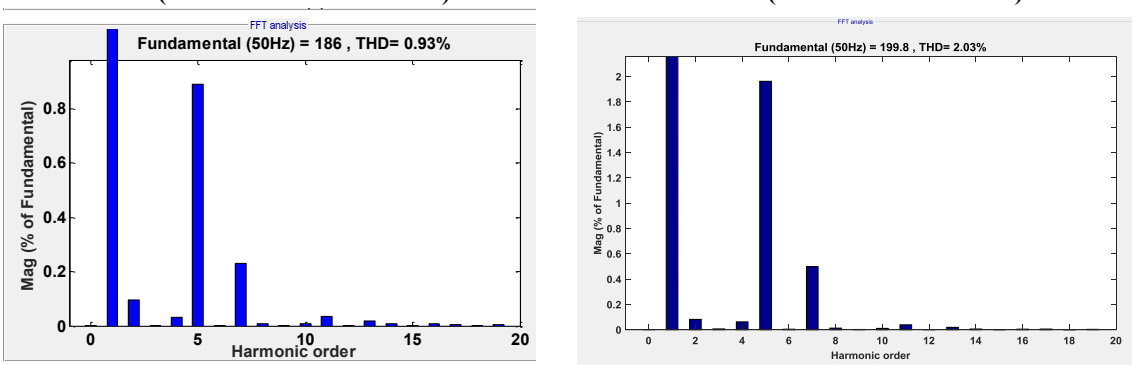

Fig. 11(a) FFT analysis for the load current waveform

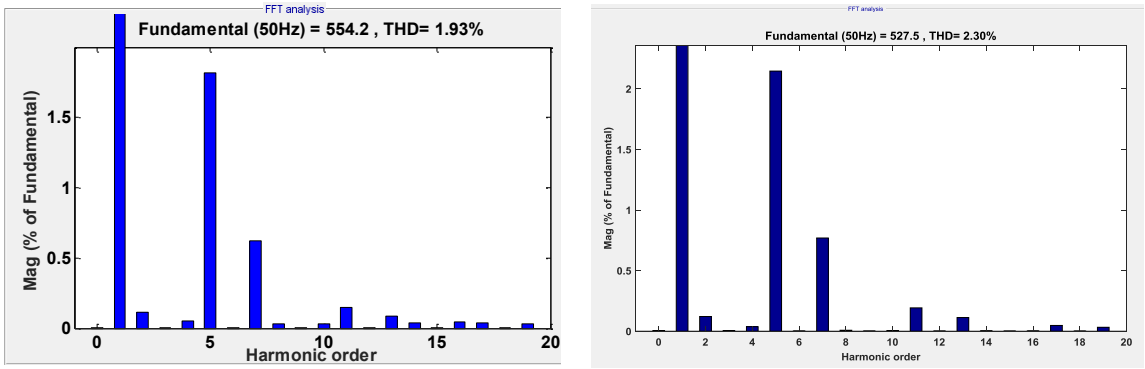

Fig. 11(b) FFT analysis for the load voltage waveform

Fig. 11. FFT analysis of current and voltage waveforms using conventional control method

Proposed Control Method

Case 1(Without non-linear load) **Case 2 (With non-linear load)**

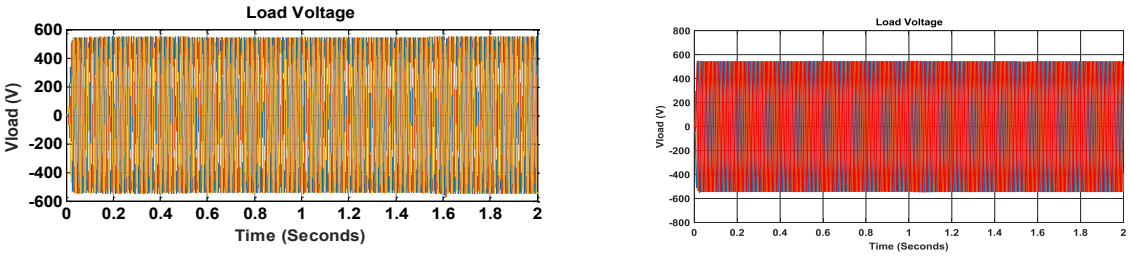

Fig. 12(a) Load voltage

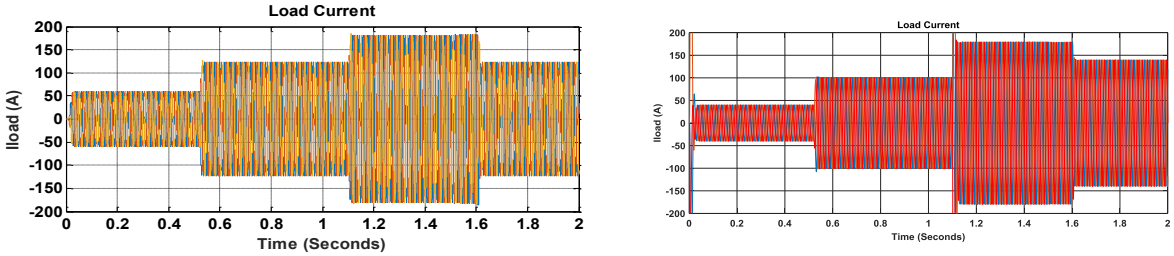

Fig. 12(b) Load current

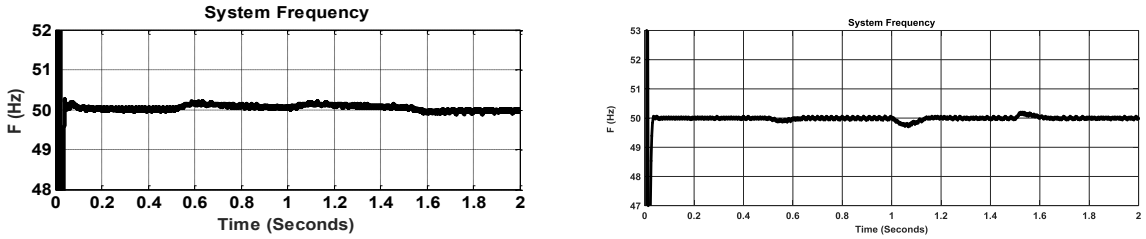

Fig. 12(c) System frequency

Fig. 12. Results for the proposed control method

Proposed Control Method

Case 1(Without non-linear load) **Case 2 (With non-linear load)**

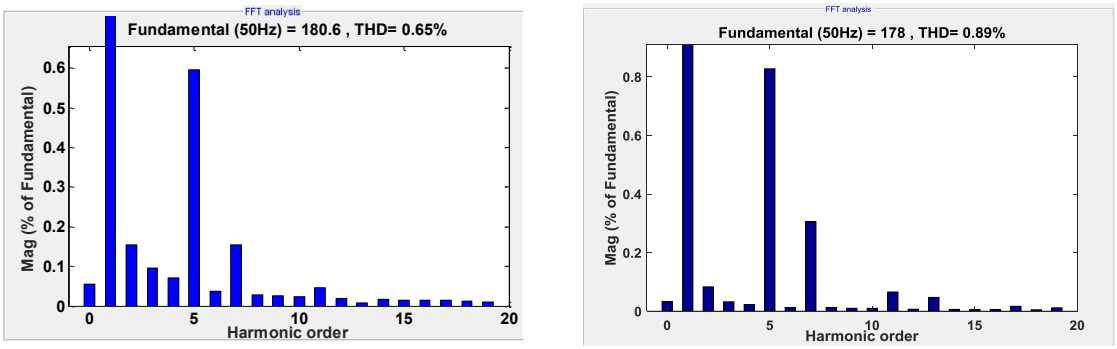

Fig. 13(a) FFT analysis for the load current waveform

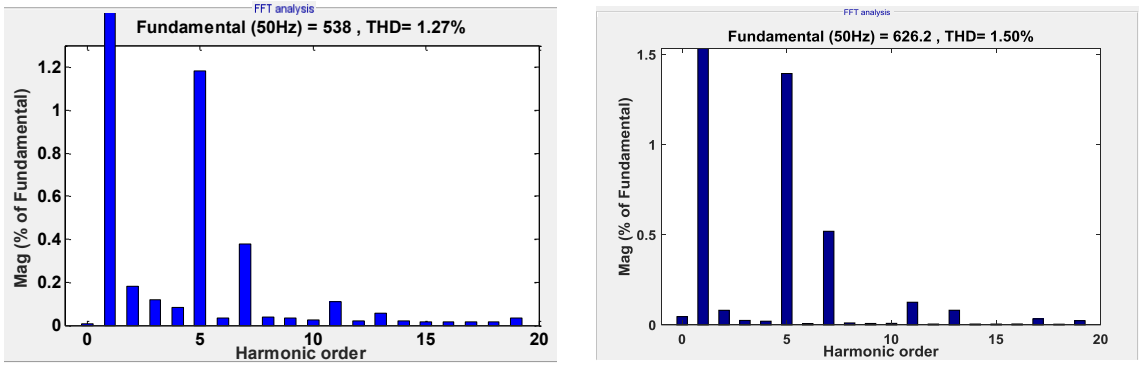

Fig. 13(b) FFT analysis for the load voltage waveform

Fig. 13. FFT analysis of current and voltage waveforms using proposed control

A comparison between the three controllers is given in Table 4. The comparison includes the THD value, the response time to load changes, and the maximum frequency jump at the system load variation instant.

Table 4. Comparison between the three controllers

Load Type	Control Method	THD (%)		Response Time (s)	Max Frequency Jump (%)
		THD_I	THD_V		
Linear Load	V/F	2.04	2.06	0.040	4.86
	Droop	0.93	1.93	0.029	4.24
	H∞	0.65	1.27	0.010	0.46
Non-Linear Load	V/F	3.85	3.16	0.052	16.74
	Droop	2.03	2.30	0.045	45.4
	H∞	0.89	1.50	0.019	0.40

The comparison shows that the proposed control method is more efficient than the two other controllers in improving the system power quality. The proposed method has the ability to reduce the THD to its minimum value under different loading conditions. The proposed controller has the shortest response time, so it can restore the system frequency to its nominal value after any variation in system load faster than the other two controllers. The proposed controller has also the lowest frequency jump compared to the other controllers in both loading conditions. In facts, the high frequency jump under non-linear loading conditions is one of the major disadvantages of the droop controllers.

Generally, the prementioned results prove that the proposed H∞ controller is more efficient and effective than both V/f and conventional controllers in adjusting the system voltage, current frequency for islanded MG during the system load variations in presence of non-linear loads. It can also improve the system power quality by reducing the THD of current and voltage waveforms.

7. Conclusion

This paper introduced an advanced control method based on H∞ controller for islanded MG. The proposed control method adjusts the system voltage and frequency and improves the system power quality. The method is a repetitive adaptive and robust control one as it uses the internal model in H∞ control and applies different weighting parameters with the H∞ control method. The method was compared with two other controllers including a base V-f controller and a conventional droop controller to explain the effectiveness and efficiency of the method. The three controllers were simulated in Matlab/Simulink environment and then applied to a test system for two case studies including two different loading conditions (linear and non-linear loads). The results proved that the proposed method restored the system voltage and frequency to their nominal values after the load violations and also improved the system power quality. The proposed controller has the lowest frequency jump compared to the other controllers in both loading conditions.

References

[1] A. Molderink, et al., "Management and Control of Domestic Smart Grid Technology", IEEE Transaction on Smart Grid, Vol. 1, 2010.

[2] H. Han, et al., "Review of Power Sharing Control Strategies for Islanding Operation of AC Microgrids", IEEE Transaction on Smart Grid, Vol. 7, 2015.

[3] J. Guerrero, M. Chandorkar, T. Lee, and P. Loh, "Advanced Control Architectures for Intelligent Microgrids—Part I: Decentralized and Hierarchical Control", IEEE Transaction in Industrial Electronics, Vol. 60, 2013.

[4] K. Rajesh, S. Dash, R. Rajagopal, R. Sridhar, "A Review on Control of AC Microgrid", Renewable and Sustainable Energy Reviews, Vol. 71, 2017.

[5] B. Eid, N. Abd Rahim, J. Selvaraj, A. El Khateb, "Control Methods and Objectives for Electronically Coupled Distributed Energy Resources in Microgrids: A Review" IEEE Systems Journal Vol. 10, 2016.

[6] T. Vandoorn, J. De Kooning, B. Meersman, L. Vandevelde, "Review of Primary Control Strategies for Islanded Microgrids with Power-Electronic Interfaces", Renewable and Sustainable Energy Reviews, Vol. 19, 2013.

[7] D. Tomislav, L. Xiaonan, C. Juan, M. Josep, "DC Microgrid – Part I: A Review of Control Strategies and Stabilization Techniques", IEEE Transactions on Power Electronics, Vol. 31, 2016.

[8] D. Olivares, et al., "Trends in Microgrid Control", IEEE Transactions on Smart Grid, Vol. 5, 2014.

[9] S. Adhikari, F. Li, " Coordinated V-f and P-Q Control of Solar Photovoltaic Generators with MPPT and Battery Storage in Microgrids", IEEE Transactions on Smart Grid, Vol. 5, 2014.

[10] N. Hajilu, et al., "Power Control Strategy in Islanded Microgrids Based on VF and PQ Theory Using Droop Control of Inverters", International Congress on Electric Industry Automation (ICEIA), Shiraz, Iran, 2015.

[11] V. Indu, E. Bindumol, "A Hybrid Photovoltaic and Battery Energy Storage System with P-Q and V-f Control Strategies in Microgrid", IEEE International Conference on Power, Instrumentation, Control and Computing (PICC), Thrissur, India, 2015.

[12] M. Hao, X. Zhen, "A Control Strategy for Voltage Source Inverter Adapted to Multi-Mode Operation in

Microgrid", 36th Chinese Control Conference, Dalian, China, 2017.

[13] S. Wu, et al., "An Intentionally Seamless Transfer Strategy Between Grid-Connected and Islanding Operation in Micro-Grid", 17th International Conference on Electrical Machines and Systems (ICEMS), Hangzhou, China, 2014.

[14] T. Nguyen, H. Yoo, H. Kim, "A Droop Frequency Control for Maintaining Different Frequency Qualities in Stand-Alone Multi-Microgrid System", IEEE Transactions on Sustainable Energy, Vol. PP, 2017.

[15] M. Savaghebi, A. Jalilian, J. Vasquez, J. Guerrero, "Autonomous Voltage Unbalance Compensation in an Islanded Droop-Controlled Microgrid", IEEE Transaction on Industrial Electronics, Vol. 60, 2013.

[16] J. Lai, et al., "Droop – Based Distributed Cooperative Control for Microgrids with Time–Varying Delays", IEEE Transactions on Smart Grid, Vol. 7, 2016.

[17] A. Solanki, et al., "A New Framework for Microgrid Management: Virtual Droop Control", IEEE Transaction on Smart Grid, Vol. 7, 2016.

[18] E. Planas, et al., "General Aspects, Hierarchical Controls and Droop Methods in Microgrids: A Review", Renewable and Sustainable Energy Reviews, Vol. 17, 2013.

[19] T. Hornik, Q. Zhong, "A Current – Control Strategy for Voltage Source Inverters in Microgrids Based on H∞ and Repetitive Control", IEEE Transactions on Power Electronics, Vol. 26, 2011.

[20] A. Sheela, S. Vijayachitra, S. Revathi, "H – Infinity Controller for Frequency and Voltage Regulation in Grid Connected and Islanded Microgrid", IEEJ Transactions on Electrical and Electronic Engineering, Vol. 10, 2015.

[21] H. Baghaee, M. Mirsalim, G. Gharehpetian, H. Talebi, "A Generalized Descriptor – System Robust H∞ Control of Autonomous Microgrids to Improve Small and Large Signal Stability Considering Communication Delay and Load Nonlinearities", International Journal of Electrical Power & Energy Systems, Vol. 92, 2017.

[22] Q. Lam, A. Bratcu, D. Riu, "Robustness Analysis of Primary Frequency H∞ Control in Stand-Alone Microgrids with Storage Units", IFAC, Vol. 49, 2016.

[23] Z. Jian, W. Chaoli, "Frequency Stability of Microgrids Based on H∞ Methods", Proceedings of the 35th Chinese Control Conference, 2016.

[24] X. Cubillos, L. de Souza, "Article Using of H-Infinity Control Method in Attitude Control System of Rigid-Flexible Satellite", Mathematical Problems in Engineering, Hindawi Publishing Corporation, Volume 2009.

[25] M. Nagahara, Y. Yomamoto, S. Miyazaki, T. Kodoh, N. Hayashi, "H∞ Control of Microgrids Involving Gas Turbine Engines and Batteries", 51st IEEE Conference on Decision and Control, Maui, HI, USA, 2012.

[26] C. Dou, F. Zhao, Z. Bo, X. Jia, D. Liu, " H∞ Robust Control of DC – AC Interfaced Microsource in Microgrids", Power Engineering and Automation Conference (PEAM), Wuhan, China, 2011 .

[27] Z. Jankovic, A. Nasiri, L. Wei, "Robust H∞ Controller Design for Microgrid – Tied Inverter Applications", Energy Conversion Congress and Exposition (ECCE), 2015.

[28] P. Li, C. Lui, W. Li, Z. Yin, J. Chen, K. Liu, "The Research on Photovoltaic Power Flexible Grid – Connected in Microgrid Based on H∞ Control", International Conference on Power System Technology (POWERCON), IEEE, Auckland, New Zealand, 2012.

[29] L. Sedghi, A. Fakharian, "Robust Voltage Regulation in Islanded Microgrids: A LMI Based Mixed H2/H∞ Control Approach", 24th Mediterranean Conference on Control and Automation, Athens, Greece, 2016.

[30] Q. Lam, A. Bratcu, D. Riu, J. Mongkoltanatas, "Multi – Variable H – Infinity Robust Control Applied to Primary Frequency Regulation in Microgrids with Large Integration of Photovoltaic Energy Source", International Conference on Industrial Technology (ICIT), IEEE, 2015.

[31] T. Hornik, Q. Zhong, " H∞ Repetitive Voltage Control of Grid – Connected Inverters with a Frequency Adaptive Mechanism", IET Power Electronics, Vol.3, 2010.

[32] T. Chaer, L. Rambault, J. Gaubert, "Electrical Energy Quality: Modeling and H∞ Control of a Three-Phase Shunt Active Filter", International Journal of Control, Automation, and Systems, Vol. 10, 2012.

[33] P. Basak, S. Chowdhury, S. Halder, S. Chowdhury, "A Literature Review on Integration of Distributed Energy Resources in the Perspective of Control Protection and Stability of Microgrid", Renewable and Sustainable Energy Reviews, Vol. 16, 2012.

[34] A. Reznik, M. Simöes, A. Al-Durra, S. Muyeen, "LCL Filter Design and Performance Analysis for Grid-Interconnected Systems", IEEE Transaction on Industrial Applications, Vol. 50, 2014.

[35] IEEE Standard, "IEEE Recommended Practices and Requirements for Harmonic Control in Electrical Power Systems", IEEE Std. 519-1992, April 1993.

[36] R. Hamidia, H. Livania, S. Hosseinianb, G. Gharehpetianba, "Distributed Cooperative Control System for Smart Microgrids", Electric Power Systems Research, Vol. 130, 2016.

[37] A. Hatata, B. Sedhom, M. El-Saadawi, "A Modified Droop Control Method for Microgrids in Islanded

Mode", Nineteenth International Middle East Power Systems Conference (MEPCON), Menoufia University, Egypt, 2017.

[38] S. Hadisupadmo, A. Hadisputro, A. Widyotriatmo, "A Small Signal State Space Model of Inverter-Based Control on Single Phased AC Power Network", Internetworking Indonesia journal, Vol. 8, 2016.

[39] M. Moradi, M. Eskandari, S. Hosseinian, "Cooperative Control Strategy of Energy Storage Systems and Micro Sources for Stabilizing Microgrids in Different Operation Modes", Electrical Power and Energy Systems, Vol. 78, 2016.

[40] O. Palizban, K. Kauhaniemi, "Hierarchical Control Structure in Microgrids with Distributed Generation: Island and Grid - Connected Mode", Renewable and Sustainable Energy Reviews, Vol. 44, 2015.

[41] A. Bidram, A. Davoudi, F. Lewis, J. Guerrero, "Distributed Cooperative Secondary Control of Microgrids Using Feedback Linearization", IEEE Transactions on Power Systems, Vol. 28, 2013.